Optimal Trajectory Design of a Satellite Moon Landing with Coasting using the Pseudospectral Method

Kegan Kawamura, Yamada Katsuhiko

Abstract

SLIM is a spacecraft that will be deployed by JAXA to land on and study the moon. The use of its novel image processing technique will provide it greater freedom for landing, but in return it will require the spacecraft to coast while landing, which means that it will follow a trajectory without using any control maneuvers. This study attempts to analyze the effects of coasting on SLIM's optimal trajectory. Using GPOPS-II, an optimization program that employs the pseudospectral method, we were able to produce a full, optimal trajectory that includes one coasting phase, and some success with a trajectory with two coasting phases. We found that with more coasting, the final downrange, peak radius, and fuel consumption all increased. In the future, we hope to expand on this research by making it possible to obtain trajectories with multiple coasting phases.

1 Introduction

Outer space is a hostile environment for explorers. Resources are extremely limited, and communication with Earth becomes difficult as one explores further out. Nevertheless, humanity has chosen to venture out into space to become a little closer to our universe. To make this possible, it is necessary to study the orbits and maneuvers that allow spacecrafts to transfer from point A to point B with the limited resources it has.

SLIM (Smart Lander for Investigating Moon) is a spacecraft developed by JAXA that will demonstrate a novel technique for landing on the moon [1]. SLIM will utilize an onboard camera to process images of the moon surface before landing in order to find safe areas to land on. However, there is one limitation to this: SLIM must turn off its main thrusters in order for it to observe the lunar surface. With SLIM moving through space without using any control maneuvers, which we will refer to as coasting, the trajectory it takes will significantly differ from the optimal one. Coasting has not been utilized often in past spacecraft, and its effects are still relatively uncertain when added to an optimal trajectory.

1.1 Goal Statement

This study explores whether it is possible to obtain a reasonable, optimal trajectory (minimum fuel consumption) that explicitly includes coasting, and analyzes how these trajectories compare to the trajectory that does not explicitly include coasting as a constraint. "Coasting" in this paper refers to a spacecraft following a trajectory without using any fuel whatsoever, allowing the craft to freely move through space without control. The coasting phase(s) will start and end as a function of time.

The study will base its research on Takehiro Higuchi's previous study on coasting [2], and will attempt to replicate and expand upon it by creating a full trajectory optimization of the spacecraft. rather than just a small portion of it. This will lead to a fuller understanding of the effects of coasting on a spacecraft, and how the trajectories may need to be modified depending on the coasting constraints.

2 Methods

Optimization is performed through a direct method called the pseudospectral method on two separate optimization computer programs: IPOPT and GPOPS-II.

2.1 The Pseudospectral Method

The pseudospectral method turns an optimal control problem into a non-linear program by discretizing the equations that define the problem. The state and control variables are approximated as functions of time by constructing them with Lagrange polynomials at the discretized points

$$\mathbf{x}(t) \approx \mathbf{x}^N(t) = \sum_{l=0}^{N} \mathbf{x}(t_l)\phi_l(t) \tag{1}$$

$$\mathbf{u}(t) \approx \mathbf{u}^N(t) = \sum_{l=0}^{N} \mathbf{u}(t_l)\phi_l(t) \tag{2}$$

N is the order of the polynomial used to approximate the function, t_l is the discretized time, with $l = 0, 1, \ldots, N$, and $\phi_l(t)$ is an orthogonal, Lagrange polynomial (such as the Legendre or Chebyshev polynomial) of order l with the following property.

$$\phi_l(t_k) = \begin{cases} 1 & l = k \\ 0 & l \neq k \end{cases} \tag{3}$$

This study used the Legendre polynomial for all optimizations. The Legendre polynomial is described by the differential equation in 4 and the Lagrange polynomial is constructed from it, described in equation 5.

$$\frac{d}{dt}\left[(1-t^2)\frac{d}{dt}L_N(t)\right] + N(N+1)L_N(t) = 0 \tag{4}$$

$$\phi_l(t) = \frac{1}{N(N+1)L_N(t)} \frac{(t^2-1)\dot{L}_N(t)}{t - t_l} \tag{5}$$

Furthermore, the pseudospectral method transforms the independent variable used (in most cases time) such that it lies in the domain $[-1, 1]$ (equation 6), and discretizes the problem at special collocation points defined by the orthogonal polynomial used. This study employed Legendre-Gauss-Lobatto points and the Legendre-Gauss-Radau points.

$$\tau = 2\frac{t - t_0}{t_f - t_0} - 1 \tag{6}$$

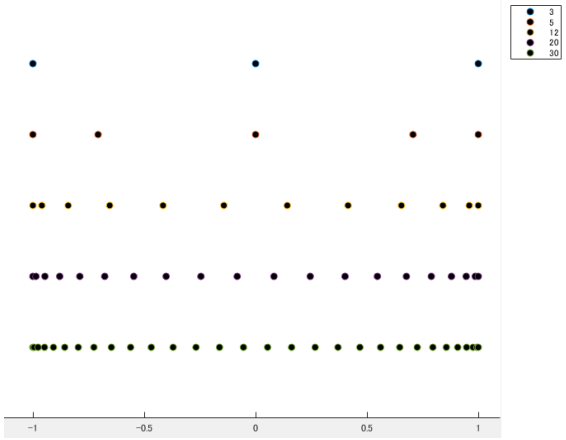

Figure 1: The discretization of time at the Legendre-Gauss-Lobatto points of several orders of magnitude.

$$\begin{aligned} \text{LGR:} \quad & L_N(\tau_l) + L_{N-1}(\tau_l) = 0 \\ \text{LGL:} \quad & \dot{L}_{N-1} = 0 \\ & \tau_0 = -1 \\ & \tau_N = 1 \end{aligned}$$

After discretizing the state and control variables, constraints are applied to the equalities and inequalities to solve the optimization.

2.2 Problem Setup and Model

A spacecraft, treated as a point mass, is modeled in two dimensions with a thruster that can be pointed in any direction. There are six state variables and two control variables.

$$\mathbf{x} = \begin{bmatrix} r \\ \theta \\ m \\ v_r \\ v_\theta \\ \beta \end{bmatrix} \qquad \mathbf{u} = \begin{bmatrix} u \\ \dot{\beta} \end{bmatrix}$$

β may have been considered a control variable, but by bounding the derivative of β instead, it became possible to obtain a much smoother output for β. Furthermore, unlike the thruster strength which can be modeled fairly accurately with discontinuities, β must be continuous in order to be realistic.

Very broadly speaking, the maneuver was separated into a transfer phase and a landing phase. The initial and final conditions for the transfer phase are listed in table 1, and for the landing phase in table 2.

The dynamics and constraints were were modeled after Park's paper [3]. A rotating frame was used as the frame of reference such that the frame rotated at the same rate as the moon (which we will refer to as ω_m. Although a few constraints varied from simulation to simulation, most of them stayed constant and are the following.

The state equations:

$$\dot{r} = v_r \tag{7}$$

$$\dot{\theta} = \frac{v_\theta}{r} \tag{8}$$

$$\dot{m} = -\frac{u}{I_{sp} g} \tag{9}$$

$$\dot{v_r} = -\frac{GM}{r^2} + \frac{u \sin(\beta)}{m} + \frac{v_\theta^2}{r} + 2\omega_m v_\theta + r\omega_m^2 \tag{10}$$

$$\dot{v_\theta} = \frac{u \cos(\beta)}{m} - \frac{v_\theta v_r}{r} - 2\omega_m v_r \tag{11}$$

$$\dot{\beta} = \dot{\beta} \qquad (\dot{\mathbf{x}}(6) = \mathbf{u}(2)) \tag{12}$$

Maximum and minimum values:

$$\begin{aligned} 0 \le t &\le 2\pi\sqrt{\frac{a_0^3}{GM}} \\ R_m + 3 \le r &\le 2(R_m + 15) \\ 0 \le \theta &\le 2\pi \\ 10 \le m &\le 302.4 \\ -\sqrt{\frac{2GM}{R_m}} \le v_r &\le \sqrt{\frac{2GM}{R_m}} \\ -1.69204 \le v_\theta &\le 2(1.69204) \\ -6\pi \le \beta &\le 6\pi \\ 0 \le u &\le u_{max} \\ -0.1 \le \dot{\beta} &\le 0.1 \end{aligned}$$

The radius of the moon is set to $R_m = 1738.4$km, the specific impulse is set to $I_{sp} = 320$, and the maximum thrust is modeled as a function of mass as $u_{max} = (6.7972 \times 10^{-4} m^2 + 0.15946m + 324.756)/1000$ [2].

2.3 Multi-phase optimization

As the problem required internal point constraints, the transfer phase was split into several subphases to specify different constraints. Higuchi's simulations include only two different kinds of phases: a coasting phase and maximum thrust

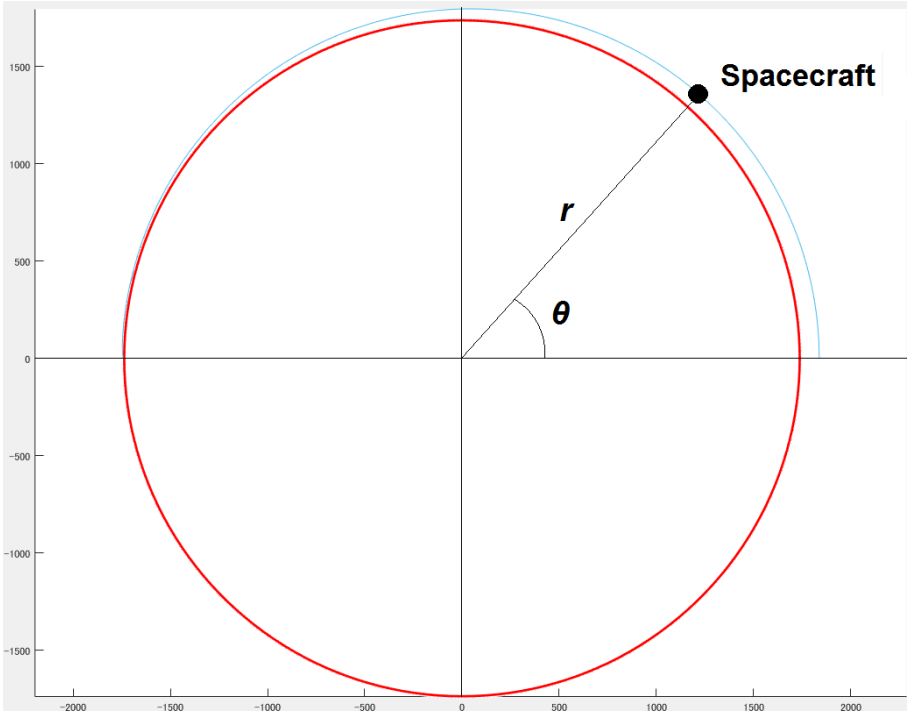

Figure 2: A model of the spacecraft relative to the moon.

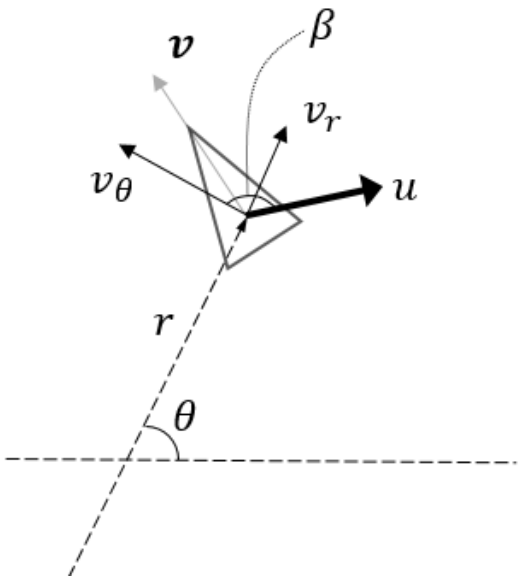

Figure 3: A model of the spacecraft and its state and control variables

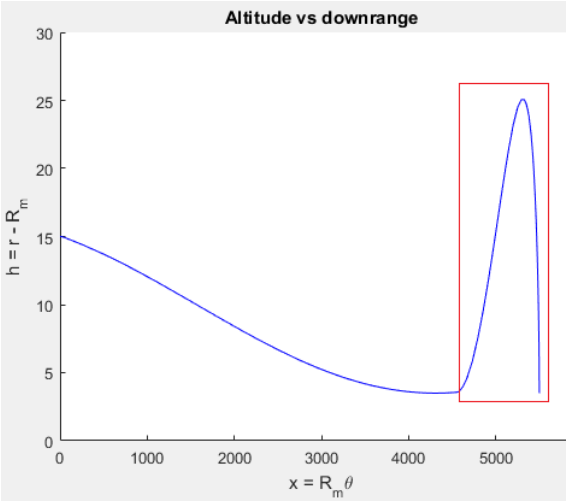

Figure 4: The trajectory of the spacecraft with no coasting. The portion covered by the square is the pre-descent subphase.

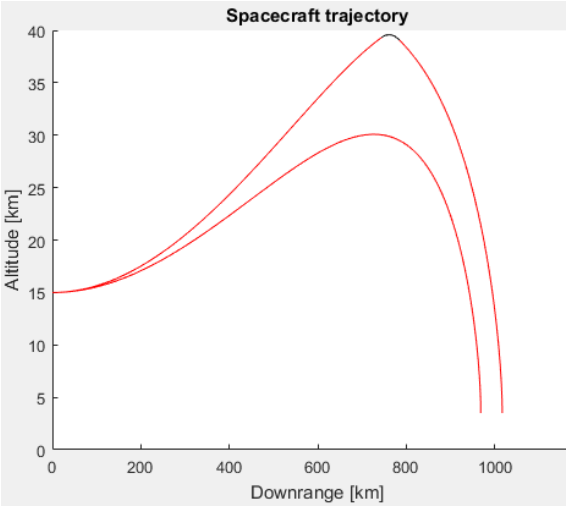

Figure 5: A reconstruction of Higuchi's simulations. The red portion is where the spacecraft is using its thrusters at maximum, and black is where it coasts. This graph shows a no coasting trajectory and a one coast trajectory.

phase. Therefore, his simulations with one coasting phase were split as thrust-coast-thrust, and his simulations with two coasting phases were split as thrust-coast-thrust-coast-thrust. A reconstruction of his results can be seen in figure 5. This is because his simulations only included the portion of the transfer phase where the spacecraft was preparing to enter its landing phase, which we show in figure 4. We will refer to this subphase as the pre-descent subphase.

When performing our own optimizations over the whole trajectory, it was found that Higuchi's use of maximum thrust for his simulations were a fair assumption. The thrust profile over time followed a max-zero-max pattern. The first max slowed the spacecraft down such that the spacecraft slowly approached the moon over time. After a long period of coasting (which is part of the optimal trajectory), the spacecraft blew its thrusters again at maximum force, creating a huge arc with its trajectory and finally reaching the terminal values of the transfer phase.

Assuming this thrust pattern to hold for all optimal trajectories, we split the transfer phase into four subphases for one coasting phase: *variable thrust - max thrust - coast - max thrust*. This will allow the optimization software to find the optimal trajectory with the coasting forced inside the pre-descent subphase, which will now consist of the *max thrust - coast - max thrust* subphases. To prove that this setup will still produce a similar optimal trajectory, we opti-

Variable	**Symbol**	**Initial**	**Final**
Radius	r [km]	$R_m + 15$	$R_m + 3$
Angle	θ [rad]	0	FREE
Mass	m [kg]	302.4	FREE
Radial Velocity	v_r [km/s]	0	-0.04
Azimuthal Velocity	v_θ [km/s]	1.69204	0
Thruster Direction	β [rad]	π	$\pi/2$

Table 1: The Initial and Final Conditions of the transfer phase

Variable	**Initial**	**Final**
r [km]	$R_m + 3$	$R_m + 0.003$
θ [rad]	$\theta_0 =$ FREE	$\theta_f = \theta_0$
m [kg]	FREE	FREE
v_r [km/s]	-0.04	0
v_θ [km/s]	0	0
β [rad]	$\pi/2$	$\pi/2$

Table 2: The Initial and Final Conditions of the landing phase

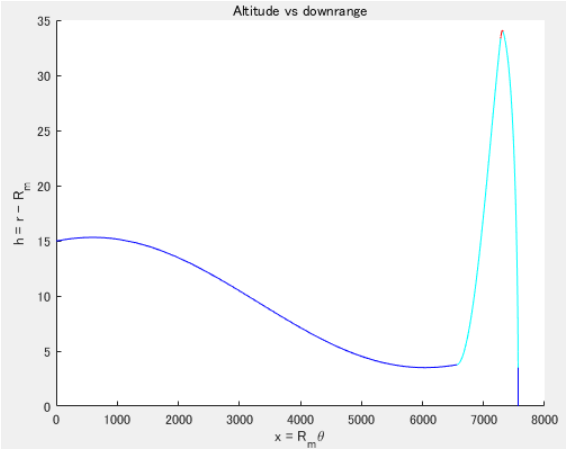

Figure 6: The altitude vs downrange graph for the optimal, one coasting trajectory.

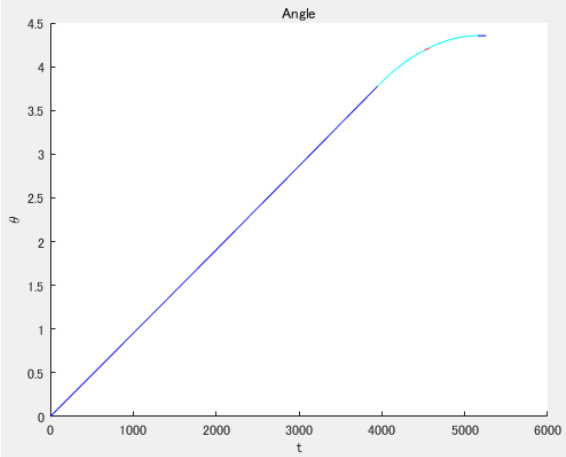

Figure 7: The θ vs t graph for the optimal, one coasting trajectory.

mized the trajectory with a *variable thrust - max thrust* subphase pattern (no coasting). The final trajectory was nearly indistinguishable from the trajectory with no subphases (just variable thrust throughout the transfer phase).

3 Results

Optimization was initially performed on IPOPT, but performance was poor when attempting to optimize on a multi-phase problem. Therefore, all successful optimizations with multiple phases was performed on GPOPS-II.

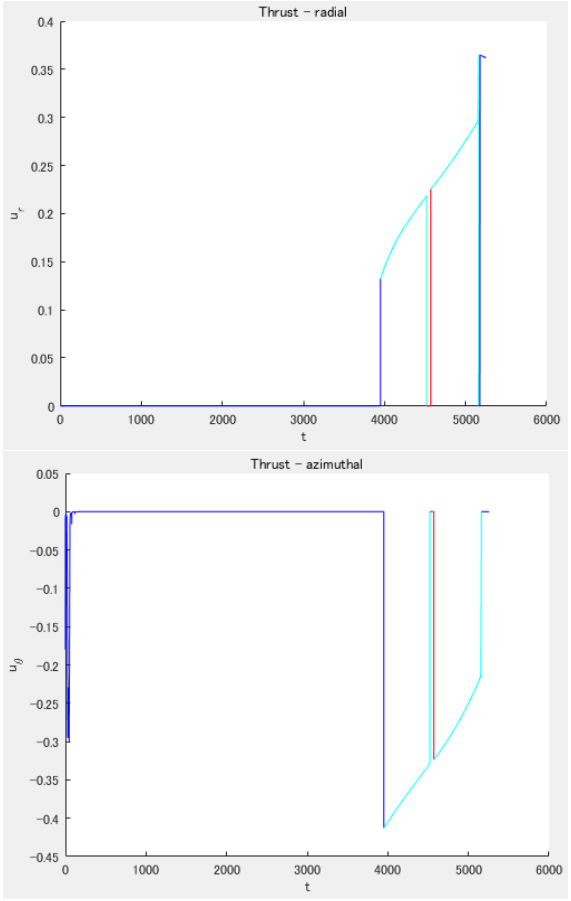

Figure 8: The control maneuvers for the optimal, one coasting trajectory.

3.1 One coasting phase

Reflecting Higuchi's simulation, we included a coasting phase of 50 seconds in the pre-descent subphase. In order to keep it right in the middle of the subphase, we added a time constraint for the two *max thrust* subphases that sandwich the *coast* subphase such that their lengths are within 20 seconds of each other. In other words, we added a soft constraint such that the length of time they each take are equivalent. By doing this, we force the coasting subphase to be right in the middle of the pre-descent subphase.

Generally speaking, when coasting was included in the optimization, the final landing θ became larger, and the peak radius increased. Furthermore, the amount of fuel consumed increased slightly. Several simulations were ran with different lengths of time for coasting, and the final θ, peak radius, and fuel consumed all increased with time. This effect can be explained

by the following. As the spacecraft coasts, it needs additional height and velocity to float above the ground before it can begin using its thrusters again, causing the increased final θ and peak radius. Furthermore, the additional fuel consumed is expected since the trajectory is straying away from the optimal one.

3.2 Two coasting phases

Coasting twice was also attempted, with mixed results. This simulation included six subphases, and had the following pattern: *variable thrust - max thrust - coast - max thrust - coast - max thrust*. Both coasting phases are 50 seconds long. The first has the same constraints as the one coasting trajectory, where the subphases that sandwich it are about the same length of time. The second coasting phase also mirrors Higuchi's simulation such that the coasting is included at some point in the last 125 seconds of the transfer phase(this was later changed to having the coasting beginning 75-175 seconds before the end of the transfer phase, in order to make the problem more feasible).

The optimization process became increasingly difficult with the introduction of the additional coasting phase, due to the mesh error not meeting within the tolerance values. This may be due to the new combination of constraints made by adding the phases for a second coasting. It is possible that the lack of a final constraint for θ will allow for multiple solutions. Evidence for this was seen when one set of initial conditions and constraints caused the spacecraft to land almost immediately, while another caused it to land on the other side of the moon (figure 9). When multiple solutions are locally optimal, the algorithm may have trouble converging to a single solution. Furthermore, adding the second coasting phase will only make the problem closer to one that is infeasible. This is especially true as the coasting approaches the end of the transfer phase, since there will be less control for the trajectory to meet the terminal conditions. Although an optimal solution is found even with two coasting phases, the solution tends to be very noisy, and we cannot conclude that it is a reasonable control maneuver (figure 10) . Regardless, as expected, the trajectories followed the same pattern as before: more coasting leads to more fuel consumption and a slower landing.

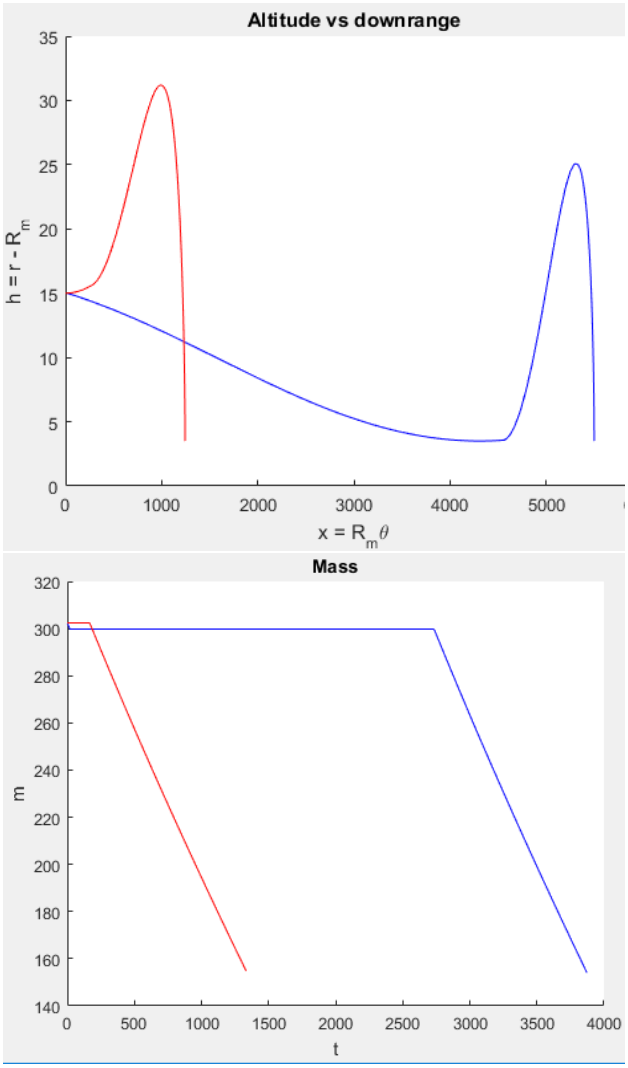

Figure 9: An example of the problem having multiple optimal solutions. The red, shorter trajectory uses a t_f initial guess of 0.2, while the blue, longer one uses an initial guess of 0.5.

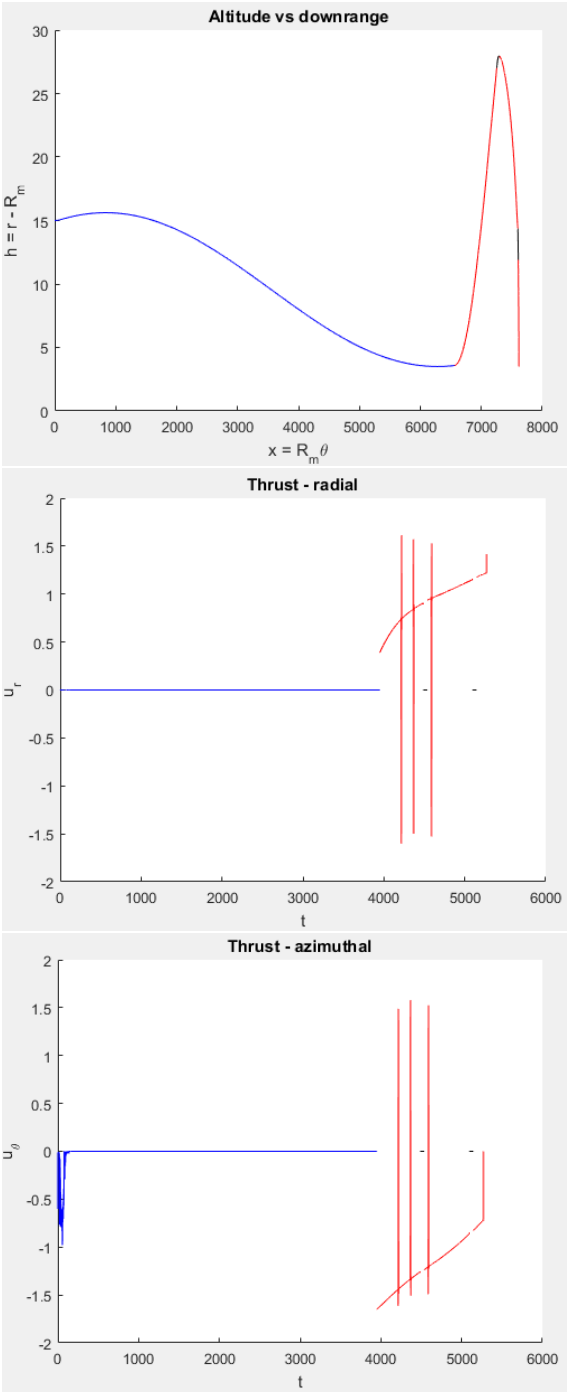

Figure 10: The noisy solution of the two coast trajectory. Although there is noise, it is still possible to make out the intended solution.

4 Conclusion

Optimization of spacecraft trajectories is an important process in extraterrestrial missions. When a spacecraft like SLIM needs to stray from its optimal trajectory, it is important to analyze how its new trajectory will affect the outcome of its mission. This study attempted to analyze the effects of coasting in the pre-descent subphase of the optimal trajectory for landing on the moon. We attempted to reproduce Takehiro Higuchi's work with SLIM, and expand upon it by creating a more full simulation of the spacecraft trajectory. By setting the appropriate initial and final conditions, and splitting the trajectory into multiple phases, trajectory optimization was performed via the pseudospectral method. We successfully reproduced Higuchi's work using GPOPS-II, and the full optimal trajectory for one coasting phase. However, the optimization became significantly difficult with two coasting phases. We can expect that with each additional coasting phase we include, the trajectory optimization will become more and more difficult. However, all simulations followed the general pattern that more coasting leads to an overall longer, final downrange for landing, a higher peak radius, and higher fuel consumption.

Future work may include further refinement of the problem to obtain reasonable results for a trajectory with more than one coasting phase. It is important to identify the underlying problem that is keeping the solution from converging well. In addition, being able to perform the optimization on IPOPT will introduce a new degree of freedom, and may be worth pursuing. Finally, it may be worthwhile to attempt to translate the results into an actual control algorithm for the lunar spacecraft.

List of Figures

List of Tables

References

[1] SLIM Homepage, `http://www.isas.jaxa.jp/home/slim/SLIM/toppupeji.html`

[2] Takehiro Higuchi, Seiya Ueno, Yuta Kimura. *Optimal Trajectory of Powered Descending Phase with Coasting for Smart Lander for Investigating Moon*, 60th Space Sciences and Technology Conference, 3C09 (JSASS-2016-4380), 2016.

[3] Bong-Gyun Park, Jong-Sun Ahn, Min-Jea Tahk. *Two-Dimensional Trajectory Optimization for Soft Lunar Landing Considering a Landing Site* International Journal of Aeronautical & Space Sciences, 12(3), 288-295, 2011.